

Short Communication

Influence of Supporting Electrolyte on the Electrocatalysis of CO₂ Reduction by Cobalt Protoporphyrin

Jing Shen^{*}, Donghui Lan, Tingjiao Yang

Department of Chemistry, College of Chemistry and Chemical Engineering, Hunan Institute of Engineering, Xiangtan 411104, Hunan, China

^{*}E-mail: jingshen84@sina.com

Received: 3 June 2018 / Accepted: 30 July 2018 / Published: 1 September 2018

The electrochemical conversion of CO₂ into high-value fuels is a promising technique to reduce CO₂ emission and relief the crisis of fossil fuel depletion. Here we report the influence of supporting electrolyte on the electrochemical reduction of carbon dioxide catalyzed by cobalt protoporphyrin. Phosphate anion strongly coordinates to the cobalt center leading to the positive movement of Co^{III}/Co^{II} redox peak and the difficulty formation of carbon monoxide. Alkali cations, such as Li⁺, Na⁺ and K⁺, exhibit different catalytic activity and product selectivity. The efficiency of the hydrogen evolution reaction from direct proton (H⁺) reduction is increasing with the increase of the cation size. That is because the smaller cations preserve larger hydration number of water leading to geometrical hindrance, which hinders the diffusion of H⁺ to the electrode surface. On the contrary, the formation of CO and CH₄ is decreasing with increasing of the cation size. This is resulted from the coordination of alkali cations to the oxygen atom of the key intermediate of CO₂ electrochemical reduction, CO₂^{-•} anion, through ion-pairing. The smaller the cation size is, the stronger the ion-pairing is, helping the cleavage of one of the C-O bond. The deeper insight into the ionic effects and reaction mechanism of the electrochemical reduction of CO₂ suggest new strategies for the utilization of CO₂.

Keywords: Cobalt protoporphyrin, CO₂ electrochemical reduction, alkali cations, phosphate

1. INTRODUCTION

Carbon dioxide is considered to be the main component of “warm-house” gases leading to seriously environmental problems in the contemporary era. With the development of industry and population expansion, carbon dioxide emission increases dramatically every year. The climate changes as the carbon dioxide concentration in the atmosphere increase having threatened the living

environment of mankind. Therefore, it has drawn worldwide interest in developing an environmentally benign process to utilize CO₂. Among all kinds of methods, the electrochemical reduction of CO₂ is a promising technique which could not only convert CO₂ using electricity produced from intermittent energy, such as wind, solar and tide, to achieve zero-carbon emission, but also produce valuable products, such as CO, HCOOH, CH₄, C₂H₄ etc. [1-5], which can be used as raw materials or fuels.

However, CO₂ is electrochemically inert and requests high energy for the first electron injection which is considered to be the rate-determining step in the electrochemical reduction of CO₂. The standard potential of the CO₂/CO₂⁻ couple is indeed as negative as -2.2 V vs SCE in an aprotic solvent such as *N,N'*-dimethylformamide (DMF) containing a counter cation (Net₄⁺) [6]. The appropriate homogeneous molecular catalysts or heterogeneous electrocatalysts have been utilized to catalyze the reaction. The widely investigated molecular catalysts include transition metal phosphine complexes, metal complexes with bipyridine ligands, metal porphyrins, phthalocyanine and cyclam [7-10]. Based on the products formed from the electrochemical reduction of CO₂, metal catalysts have been divided into different groups. Among all metal catalysts, Cu is the most exceptional one which gives CH₄, C₂H₄ and alcohols as main products [11-13]. The catalytic activity of catalysts and product distribution are significantly affected by the characteristics of supporting electrolyte. Electrochemical reduction of CO₂ and CO was conducted with a copper electrode in hydrogen carbonate solutions with various cations by Hori and coworkers [14]. They found that the product selectivity was influenced by cationic species of aqueous electrolyte. Hydrogen evolution reaction was dominant in Li⁺ electrolyte, while CO₂ reduction was favorable in Na⁺, K⁺ and Cs⁺ solutions. Furthermore, the ratio of C₂H₄ to CH₄ became larger with increase of cation size (i.e., in the order of Li⁺ < Na⁺ < K⁺ < Cs⁺). Zhou and coworkers studied the effects of the electrolyte in terms of the nature of the cations, anions and their concentrations to understand how they affect the selectivity and faradic efficiency of formic acid from CO₂ electrochemical reduction on Sn electrode [15]. Savéant and coworkers investigated the synergistic effect of weak Brønsted acids and Lewis acid cations on the electrochemical reduction of CO₂ catalyzed by iron(0) tetraphenylporphyrins [16, 17]. They claimed that iron-CO₂ adduct was the key intermediate which is stabilized by H-bonding or ion-pairing of Brønsted acids or Lewis acid cations respectively. The resulting adduct was more prone to cleave one of the C-O bonds with the synergistic effect. The electrochemical reduction of CO₂ at Cu electrode in methanol-based electrolyte was explored by Ohta and coworkers using sodium supporting salts and other alkali salts [18]. They found that the main products were methane, ethylene, carbon monoxide and formic acid from CO₂ reduction. Besides, the selectivity depended remarkably upon both cationic and anionic species.

In this study, the electrochemical reduction of CO₂ at a cobalt protoporphyrin immobilized pyrolytic graphite (PG) electrode with various supporting electrolyte has been investigated. The effect of the anionic and cationic species on the catalytic activity and produce selectivity has been discussed. Despite the lack of the faradic efficiency data, this work triggers a deeper understanding of the mechanism of CO₂ electrochemical reduction catalyzed by porphyrin molecular catalyst. The valuable results can contribute to a large-scale manufacturing of useful chemicals from a huge amount of CO₂ as raw material.

2. EXPERIMENTAL

2.1 Electrochemistry

The electrochemical experiments were conducted in a one-compartment three-electrode cell, equipped with a home-made pyrolytic graphite (PG) electrode as working electrode, a Pt wire as counter electrode, and a reversible hydrogen electrode (RHE) as reference electrode which all potentials were referred to in this article. An Ivium potentiostat/galvanostat (Ivium Stat) was used for all electrochemical experiments. A concentrated sulfuric acid and nitric acid mixture was utilized to clean all glassware, which was then boiled in Milli-Q water (Milli-Q gradient A10 system, 18.2 M Ω cm) for 5 times before every experiment. Cyclic Voltammetry (CV) was utilized to confirm successful immobilization of cobalt protoporphyrin on PG electrode. As shown in the literature [19], Co^{III}/Co^{II} transition presents a redox peak at 0.82 V.

2.2 Preparation of cobalt protoporphyrin immobilized pyrolytic graphite electrode

0.5 mM cobalt protoporphyrin (Frontier Scientific) solution was prepared as in the literature [19]. 8 mg of cobalt protoporphyrin was dissolved in 25 mL of a 0.01 M sodium borate (Sigma-Aldrich), whose pH was adjusted to 10 by adding NaOH (Sigma-Aldrich, 99.998%). The PG electrode was abraded by P500 and P1000 SiC sandpaper and subsequently ultrasonicated in Milli-Q water for 1 min. The cobalt protoporphyrin immobilized PG electrode was prepared by dipping dried PG electrode into cobalt protoporphyrin solution for 5 min. Before using for electrochemical experiments, the electrode was rinse with water.

2.3 OLEMS measurements

The volatile products of the electrochemical reduction of CO₂ catalyzed by cobalt protoporphyrin were measured using online electrochemical mass spectroscopy (OLEMS) equipped with an evolution mass spectrometer system (European Spectrometry system Ltd) [20]. All the gaseous products were collected into the mass spectrometer through a polyether ether ketone (PEEK) capillary using porous Teflon tip (inner diameter, 0.5 mm) with a pore size of 10-14 μ m. Before experiments, the tip was immersed in a 0.2 M K₂Cr₂O₇ in 2 M H₂SO₄ solution for 15 min for cleaning and thoroughly rinsed with water. Then it was positioned to the center of the working electrode surface closely (~ 10 μ m) for collecting volatile products. All the detected fragments were applied a secondary electron multiplier (SEM) voltage with 2400 V except for hydrogen (m/z=2) which was 1200 V. The CV was scanning from 0 V to -1.5 V with a scan rate of 1 mV/s while OLEMS was conducted.

3. RESULTS AND DISCUSSION

3.1 Cobalt protoporphyrin immobilization

The successful immobilization of cobalt protoporphyrin on PG electrode was ascertained using CV as shown in Figure 1. In order to investigate the influence of supporting electrolyte on the adsorption properties of cobalt protoporphyrin, the cyclic voltammograms have been collected in 0.1 M phosphate buffer and perchlorate solution at pH = 3 in a potential range from 0 V to 1.3 V. $\text{Co}^{\text{III}}/\text{Co}^{\text{II}}$ transition presents a redox peak at 0.82 V in 0.1 M perchlorate solution with a relatively narrow double layer. By contrast, the redox peak of $\text{Co}^{\text{III}}/\text{Co}^{\text{II}}$ transition moves to more positive potential which is about 0.91 V in phosphate buffer. Besides, the thickness of double layer in phosphate buffer is larger than that in perchlorate solution. As illustrated in the literature [21], the anion adsorbability increases in the following order: $\text{ClO}_4^- < \text{NO}_3^- < \text{SO}_4^{2-} < \text{H}_2\text{PO}_4^-$. Therefore, we could expect higher adsorbent concentration on the electrode surface in phosphate buffer compared with that in perchlorate solution, resulting in larger thickness of double layer during electrochemical measurements. On the other hand, phosphate anions are suspected to coordinate to the catalytic metal centers of cobalt protoporphyrin molecules and make the electron transfer between cobalt center and electrode more difficult than that in perchlorate solution. Thus the potential of $\text{Co}^{\text{III}}/\text{Co}^{\text{II}}$ transition moves to more positive potential compared with that in perchlorate solution.

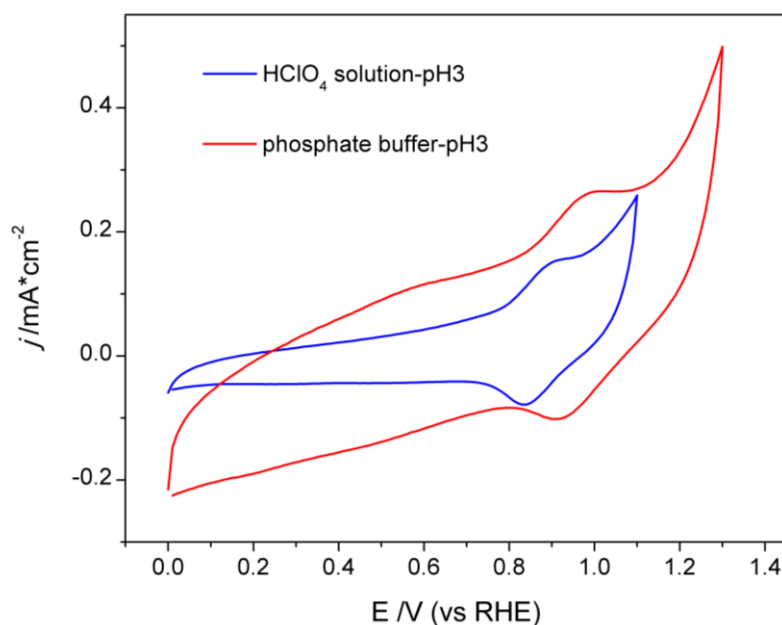
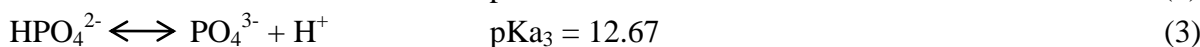
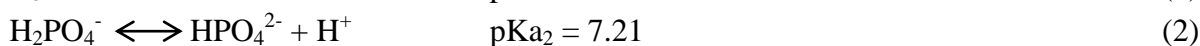
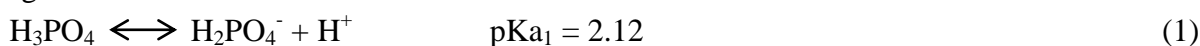


Figure 1. Influence of supporting electrolyte on the cyclic voltammetry profiles of $\text{Co}^{\text{III}}/\text{Co}^{\text{II}}$ redox peak on immobilized cobalt protoporphyrin at pH = 3. Blue line: 0.1 M perchlorate solution; Red line: 0.1 M phosphate buffer solution. Scan rates in both cases were 100 mV s^{-1} .

3.2 Phosphate effect

The hydrogen evolution is a competitive reaction with CO₂ electrochemical reduction. Therefore, it is reasonable to first understand the role of pH on the hydrogen evolution reaction by using cyclic voltammetry in the absence of CO₂ in phosphate buffer. Figure 2 shows cyclic voltammograms of the hydrogen evolution reaction in N₂ saturated phosphate buffer at different pH. The current density at pH 1 is almost 3 times as high as those at other pH and decreases in sequence as pH increasing, even though the distinction from pH 3 to pH 7 is small. The onset potentials for the hydrogen evolution reaction at different pH have been compared with as shown in insert profile. We can find that the onset potential of the hydrogen evolution reaction is about -0.6 V at pH = 1 and becomes more negative with the increase of pH. The active species in phosphate buffer for the hydrogen evolution reaction probably are H₃PO₄, H₂PO₄⁻ and HPO₄²⁻ respectively depending on pH. In order to better understand the effect of pH, pKa of phosphate anions and H₂O has been studied as following:



The comparison of pKa indicates that the highest current density at pH = 1 may come from the direct H₃PO₄ reduction which is much easier than H₂PO₄⁻ and HPO₄²⁻ species. In our previous studies [22], the onset potential of the hydrogen evolution reaction in perchlorate solution is about -0.5 V and -1.0 V related to direct H⁺ reduction and water splitting respectively. Besides, based on the comparison of pKa, we could expect lower onset potential of hydrogen evolution reaction in phosphate buffer as they all have lower pKa value than H₂O. However, it gives opposite result from cyclic voltammetry. This is probably due to the coordination of phosphate anion to the catalytic metal center of porphyrin molecules [23].

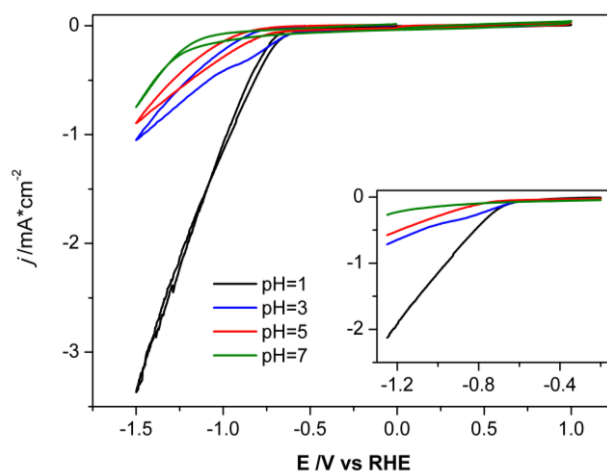


Figure 2. pH dependence of the hydrogen evolution reaction in N₂ saturated phosphate buffer at different pH. pH = 1 (black curve); pH = 3 (blue curve); pH = 5 (red cure) and pH = 7 (green curve). Inserted: zoom in the potential range from -0.2 V to -1.25 V. Scan rates in all cases were 100 mV s⁻¹.

The electrochemical reduction of CO₂ on cobalt protoporphyrin in phosphate buffer was investigated using OLEMS in different pH as shown in Figure 3. H₂ and CH₄ are the only gaseous products we can find at all pH. We also monitored the formation of CO and the consumption of CO₂ which are not shown here as there are no obvious changes during the reaction. At pH = 1, H₂ and CH₄ are produced simultaneously at the same onset potential which is about -0.6 V. By contrast, the OLEMS results exhibit similar trends for the H₂ and CO formation at pH = 3 and 5. The onset potential of the hydrogen evolution reaction (HER) (-0.6 V) is relatively more positive than that of CO₂ electrochemical reduction (-1.0 V) indicating that cobalt protoporphyrin is more catalytic active for the hydrogen evolution reaction. We can clearly find two peaks for hydrogen formation located at -0.6 V and -1.2 V respectively. As discussed in our previous work [22], we assume that the early H₂ formation probably is resulted from the direct H⁺ reduction, while the later one comes from the water splitting, even though we cannot find corresponding reduction peak in cyclic voltammograms. CH₄ is produced from the electrochemical reduction of CO₂ when the direct H⁺ reduction reaches a plateau. Based on this observation, we can legitimately speculate that H₂O is energetic sufficient for the formation of CH₄. Despite of the discrepancies in the onset potential of H₂ and CH₄ formation and the pathway of the hydrogen evolution reaction at different pH, the product distribution is not tuned by changing pH. Buffer solutions are used to keep pH at a nearly constant value. Therefore, the influence of pH is difficult to be discussed in buffer solutions. Furthermore, phosphate anion is considered to interfere with the catalytic metal center of porphyrin or the intermediates of CO₂ electrochemical reduction. It may be the other reason which hinders the detection of the role of pH. In order to avoid the interference of buffer solutions and coordinating anions, the impact of cations was investigated in perchlorate solution with different alkali cations.

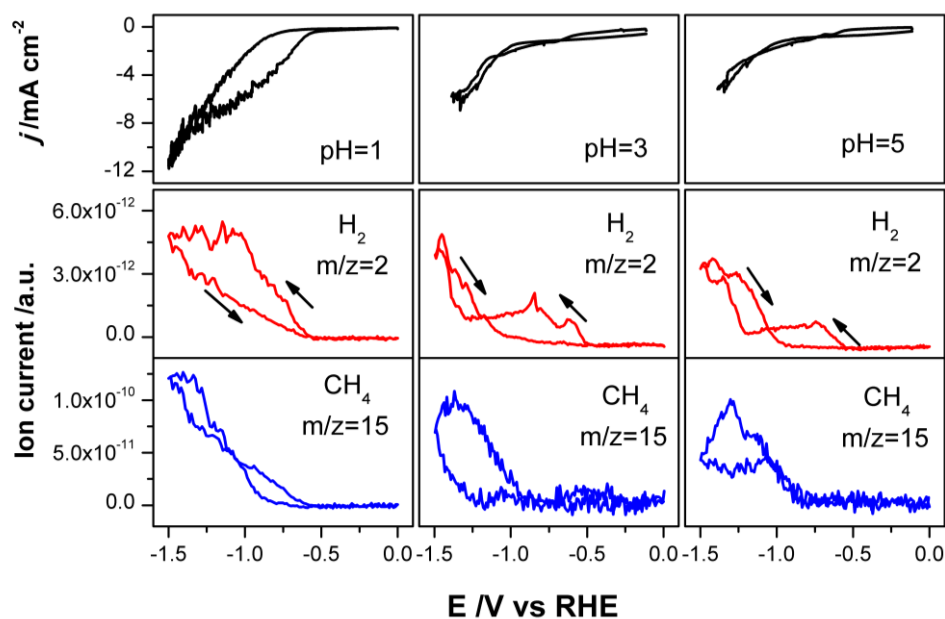


Figure 3. Influence of phosphate buffer solutions on the catalytic activity and products selectivity of the electrochemical reduction of CO₂ catalyzed by cobalt protoporphyrin at different pH. Column I: pH = 1; Column II: pH = 3; Column III: pH = 5. The arrows indicate the direction of the reaction. Scan rates in all cases were 1 mV s⁻¹.

3.3 Cation effect

The influence of cations is investigated in 0.1 M perchlorate solution consisted of 0.09 M LiClO_4 , NaClO_4 and KClO_4 respectively with 0.01 M perchlorate acid as shown in Figure 4. Compared to the electrochemical reduction of CO_2 in phosphate buffer, the most obvious difference is the distinct formation of CO in perchlorate solution. From CV measurements, the current density of CO_2 electrochemical reduction in LiClO_4 and NaClO_4 solution is almost the same, while it becomes much higher in KClO_4 solution. The current density in KClO_4 solution exhibits violent fluctuation which probably is due to the huge amount of bubbles formed during the reduction as shown in OLEMS measurements. There are two regions related to the H_2 formation which is started at -0.5 V and -1.0 V corresponding to the direct H^+ reduction and water splitting respectively. The direct H^+ reduction is significantly affected by the properties of alkali cations. The catalytic activity is increased as the cation size increasing. Therefore, we can observe that the formation of H_2 from the direct H^+ reduction is in the following order: $\text{K}^+ > \text{Na}^+ > \text{Li}^+$. On the contrary, the electrochemical reduction of CO_2 exhibits opposite trend. It is worthy to note that we do not calibrate the fragment $m/z=28$ from CO_2 signal.

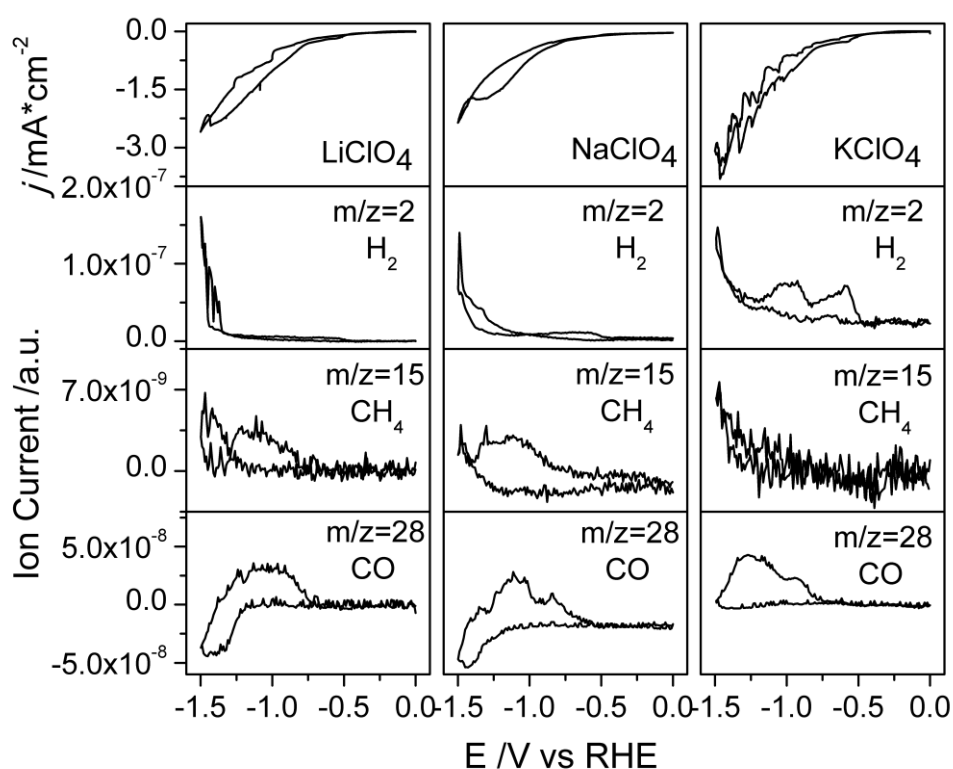


Figure 4. The electrochemical reduction of CO_2 on cobalt protoporphyrin immobilized PG electrode and the volatile products detected by OLEMS. Column I: 0.09 M LiClO_4 + 0.01 M HClO_4 ; Column II: 0.09 M NaClO_4 + 0.01 M HClO_4 ; Column III: 0.09 M KClO_4 + 0.01 M HClO_4 ; Row I: CV; Row II: fragment $m/z=2$ (H_2); Row III: fragment $m/z=15$ (CH_4); Row IV: fragment $m/z=28$ (CO). Scan rates in all cases were 1 mV s^{-1} .

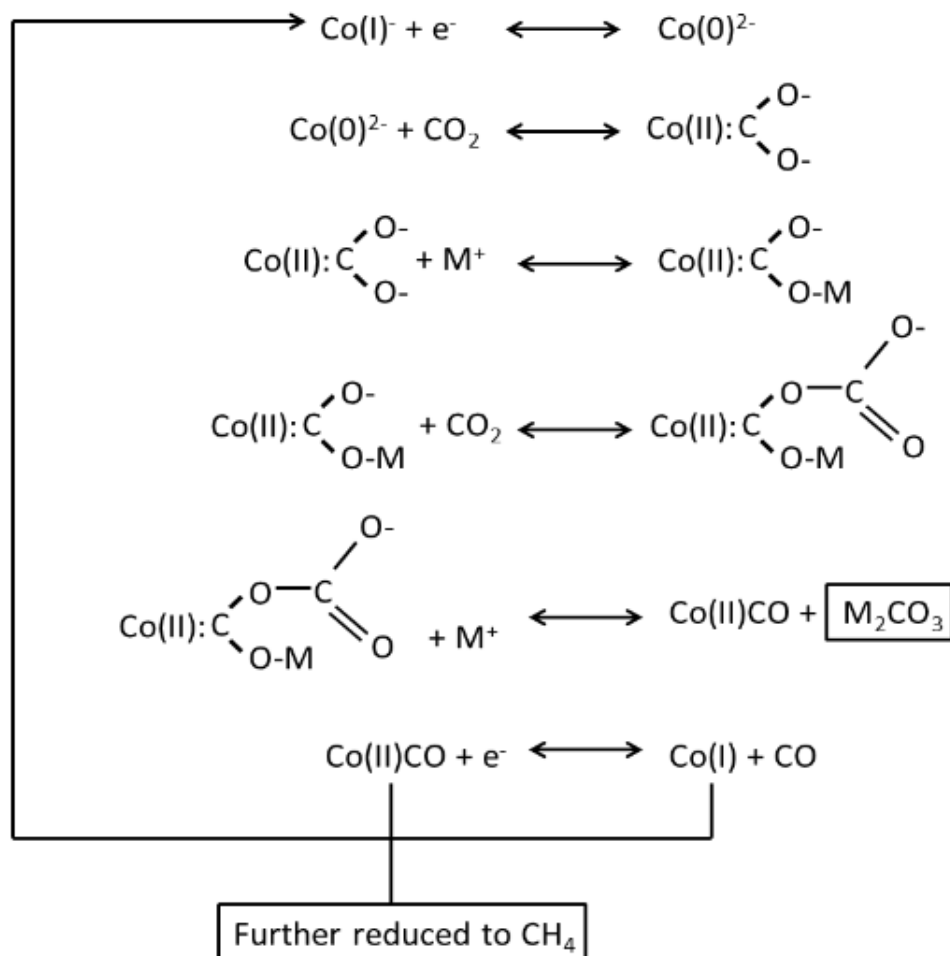
Therefore, we can observe the negative signal of CO in OLEMS measurements illustrating that massive CO_2 has been consuming. CO and CH_4 are the main products from the electrochemical reduction of CO_2 and they are started producing at almost the same potential (-0.75 V) which is more

negative than the onset potential of the hydrogen evolution reaction. When the potential scans to more negative region such as -1.2 V, the consumption of CO₂ is increased leading to negative mass signal of CO, while the formation of CH₄ is increased too. Based on the mass spectrometric results, we can speculate that CO probably is an intermediate for CH₄ formation. The catalytic activity of cobalt protoporphyrin towards the electrochemical reduction of CO₂ depends on the characterization of alkali cations. As the radius of alkali cations increase, the amount of CO and CH₄ decreases. In KClO₄ solution, CH₄ is only produced at very negative potential with tiny amount and the mass signal of CO does not go below zero indicating that there is no huge amount CO₂ consumption. In order to thoroughly discuss the effect of alkali cations, it is necessary to investigate the faradic efficiencies of all products. Unfortunately, the OLEMS measurement cannot provide quantitative analysis. Therefore, we cannot offer quantitative comparison, which will be investigated in the future.

The rate determining step in the hydrogen evolution reaction is: $H^+ + e^- \rightarrow H^\bullet$, which is diffusion limited. During electrochemical reduction, the electrode is negatively charged leading to the adsorption of cations through electrostatic attraction. Differences in the ionic radiuses of the cations employed will significant affect their adsorption status on the surface. The ionic radiuses of Li⁺, Na⁺ and K⁺ are 68, 102 and 138 pm, respectively [24]. Cations with smaller ionic radiuses have larger hydration powers. The hydration numbers of Li⁺, Na⁺ and K⁺ are 22, 13 and 7, respectively [25]. Consequently, the smaller a cation is, the bigger is its geometric configuration which causes more difficult for H⁺ diffusing to the surface of the electrode. As a result, H₂ production increases with increasing of cation size (i.e., Li⁺ < Na⁺ < K⁺).

The reaction mechanism of the electrochemical reduction of CO₂ is depicted in Scheme 1, in which the pathway leading to minor product of methane has been ignored. As illustrated in our previous work [22], CO₂ electrochemical reduction happens at the potential region where the oxidation state of cobalt center is 0. Then CO₂ will adsorb to cobalt center by electron transfer from cobalt atomic orbital to CO₂ molecular orbital leading to the formation of CO₂^{-•} anion [26-28]. After that, cations in the electrolyte will assist the further reduction through coordination with one of the oxygen atom in CO₂^{-•} anion as shown in Scheme 1. The coordination consists in a reversible ion-pairing by alkali cations, followed by the reaction with second CO₂ molecule which then irreversibly eliminates carbonate. After the elimination of carbonate, adsorbed CO intermediate is produced. It can either be released to form CO as final product or further reduced to methane. As shown in Figure 4, CO formation increases with decreasing of cation size (i.e., Li⁺ > Na⁺ > K⁺). The negatively charged CO₂^{-•} anion acts as a Lewis base which can be stabilized by Lewis acid such as alkali cations through ion-pairing. However, this is not the sole role of the Lewis acid cations, of which the main purpose is to help the breaking of one of the C-O bonds [16], thereby driving the reaction. Consequently, the stronger ion-pairing leads to higher catalytic activity and product efficiency. The smaller the ionic radius is, the easier it is to form an ion-pairing. As illustrated above, the ionic radiuses of alkali cations increase in the order: Li⁺ < Na⁺ < K⁺, leading to the opposite tendency of the CO formation (i.e., Li⁺ > Na⁺ > K⁺). The adsorbed CO intermediate could sequentially be reduced to CH₄ through a concerted proton-coupled electron transfer process in which water is energetic sufficient driving the reaction [22]. Thus, alkali cations play the same role in CH₄ formation. The synergistic effects of Lewis acid cations on the catalysis of the electrochemical reduction of carbon dioxide by Iron(0) porphyrins have been

interpreted by Savéant and co-workers. They proposed push-pull mechanisms in the catalysis of CO₂ reduction as illustrated in Scheme 1 and explicated the presence of an electron deficient synergist helping the cleavage of one of the C-O bonds. What they found is comparable to what we presented here indicating the reliability of our conclusion.



Scheme 1. The proposal of the possible reaction mechanism of the electrochemical reduction of CO₂ catalyzed by cobalt protoporphyrin.

4. CONCLUSIONS

Influence of supporting electrolyte on the electrochemical reduction of CO₂ catalyzed by cobalt protoporphyrin has been investigated. The strong coordination of phosphate anions with the metal center of porphyrin molecules is not only exhibit obvious pH dependence of the hydrogen evolution reaction, but also hinders the formation of CO. The catalytic activity for the electrochemical reduction of CO₂ is increased with decreasing of the cations radiuses (i.e., Li⁺ > Na⁺ > K⁺), while it is in an opposite order for the hydrogen evolution reaction (i.e., Li⁺ < Na⁺ < K⁺). The hydration of alkali

cations inhibits H⁺ diffusion to electrode surface by the steric hindrances. Alkali cations act as Lewis acid stabilizing the key intermediate of CO₂ electrochemical reduction, which is CO₂^{-•} anion. More important, they help to cleavage one of the C-O bond through ion-pairing, which is enhanced with smaller ionic radius. Unfortunately, the current research could not offer the quantitative measurements, which need further investigation in the future. However, this work triggers a deeper understanding on the mechanism of CO₂ electrochemical reduction and the factors tuning the catalytic activity and product selectivity on porphyrin catalyzed system.

ACKNOWLEDGEMENTS

This work was supported by the Natural Science Foundation of China (No. 21709060), the Normal Project of Hunan Province Education Department for financial support (No. 17C0391) and 2016 Talent Research Startup Fund of Hunan Institute of Engineering (No. 17RC021).

References

1. D.P. Summers, S. Leach, K.W. Frese, *J. Electroanal. Chem.*, 205 (1986), 219.
2. Y. Hori, H. Wakebe, T. Tsukamoto, O. Koga, *Electrochim. Acta*, 39 (1994), 1833.
3. C. Delacourt, P.L. Ridgway, J.B. Kerr, J. Newman, *J. Electrochem. Soc.*, 155 (2008) B42.
4. B.A. Rosen, A. Salehi-Khojin, R. Thorson, W. Zhu, D.T. Whipple, P.J.A. Kenis, R.I. Masel, *Science*, 334 (2011) 643.
5. S. Kaneco, H. Katsumata, T. Suzuki, K. Ohta, *Energy & Fuels*, 20 (2006) 409.
6. E. Lamy, L. Nadjò, J-M.J. Savéant, *J. Electroanal. Chem.*, 78 (1977) 403.
7. C. Costentin, S. Drouet, M. Robert, J-M.J. Sevéant, *Science*, 338 (2012) 90.
8. T. Atoguchi, A. Aramata, A. Kazusaka, M.J. Enyo, *Chem. Soc. Chem. Commun.*, 3 (1991) 156.
9. T. Yoshida, K. Kamato, M. Tsukamoto, T. Iida, D. Schlettwein, M. Kaneko, D. Wohrle, *J. Electroanal. Chem.*, 385 (1995) 209.
10. L.J. Chen, Z.G. Guo, X.G. Wei, C. Gallenkamp, J. Bonin, E. Anxolabéhère-Mallart, K.C. Lau, T.C. Lau, M. Robert, *J. Am. Chem. Soc.*, 137 (2015) 10918.
11. K.J.P. Schouten, Y. Kwon, C.J.M. van der Ham, Z. Qin, M.T.M. Koper, *Chem. Sci.*, 2 (2011) 1902.
12. R. Kas, R. Kortlever, H. Yilmaz, M.T.M. Koper, G. Mul, *ChemElectroChem.*, 2 (2015) 354.
13. F.S. Roberts, K.P. Kuhl, A. Nilsson, *Angew. Chem. Int. Ed.*, 54 (2015) 5179.
14. A. Murata, Y. Hori, *Bull. Chem. Soc. Jpn.*, 64 (1991) 123.
15. J.J. Wu, F.G. Risalvato, F.S. Ke, P.J. Pellechia, X.D. Zhou, *J. Electrochem. Soc.*, 159 (2012) F353.
16. I. Bhugun, D. Lexa, J.M. Savéant, *J. Phys. Chem.*, 100 (1996) 19981.
17. I. Bhugun, D. Lexa, J.M. Savéant, *J. Am. Chem. Soc.*, 118 (1996) 1769.
18. S. Kaneco, H. Katsumata, T. Suzuki, K. Ohta, *Energy & Fuels*, 20 (2006) 409.
19. M.T. De Goort, M.T.M. Koper, *Phys. Chem. Chem. Phys.*, 10 (2008) 1023.
20. A.H. Wonders, T.H.M. Housmans, V. Rosa, M.T.M. Koper, *J. Appl. Electrochem.*, 36 (2006) 1215.
21. F. Silva, A. Martins, *J. Electroanal. Chem.*, 467 (1999) 335.
22. J. Shen, R. Kortlever, R. Kas, Y.Y. Birdja, O. Diaz-Morales, Y. Kwon, I. Ledezma-Yanez, K.J.P. Schouten, G. Mul, M.T.M. Koper, *Nat. Commun.*, 6 (2015) 8177.
23. O. Diza-Morales, T.J.P. Hersbach, D.G.H. Hettterscheid, J.N.H. Reek, M.T.M. Koper, *J. Am. Chem. Soc.*, 136 (2014) 10432.
24. R. Shannon, *Acta Crystallographica Section A*, 32 (1976) 751.
25. M.E. Essington, *Soil and Water Chemistry: An Integrative Approach*, CRC Press (2004).

26. J. Shen, M.J. Kolb, A.J. Göttle, M.T.M. Koper, *J. Phys. Chem. C.*, 120 (2016) 15714.
27. I.M.B. Nielsen, K. Leung, *J. Phys. Chem. A.*, 114 (2010) 10166.
28. K. Leung, I.M.B. Nielsen, N. Sai, C. Medforteh, J.A. Shelnett, *J. Phys. Chem. A.*, 114 (2010) 10174.

© 2018 The Authors. Published by ESG (www.electrochemsci.org). This article is an open access article distributed under the terms and conditions of the Creative Commons Attribution license (<http://creativecommons.org/licenses/by/4.0/>).